Article

P-MODE OSCILLATIONS IN HIGHLY GRAVITATIONALLY STRATIFIED MAGNETIC SOLAR ATMOSPHERES

Michael Griffiths [1]*, Norbert Gyenge [6], Robertus Erdélyi [2,3,4,‡], Ruisheng Zheng [5], and Marianna Korsós [7,3,4,‡]

1 Research IT, The University of Sheffield, 10-12 Brunswick Street, Sheffield, S10 2FN, UK.; m.griffiths@sheffield.ac.uk
2 Solar Physics and Space Plasma Research Centre (SP^2RC), School of Mathematics and Statistics, University of Sheffield, Hicks Building, Hounsfield Road, S7 3RH, UK; robertus@sheffield.ac.uk
3 Dept of Astronomy, Eötvös L. University, Pázm'any Péter sétány 1/a, Budapest, H-1117, Hungary
4 Hungarian solar Physics Foundation (HSPF), Petőfi tér 3, Gyula, H-5700, Hungary
5 Shandong Key Laboratory of Optical Astronomy and Solar-Terrestrial Environment, School of Space Science and Physics, Institute of Space Sciences, Shandong University, Weihai, Shandong, 264209, China; r.zheng@sheffield.ac.uk
6 Research IT, The University of Sheffield, 10-12 Brunswick Street, Sheffield, S10 2FN, UK.; n.g.gyenge@sheffield.ac.uk
7 Dipartimento di Fisica e Astronomia "Ettore Majorana", Università di Catania, Via S. Sofia 78, I 95123 Catania, Italy ; marianna.korsos@dfa.unict.it
* Correspondence: m.griffiths@sheffield.ac.uk

Citation: Griffiths, M.; Gyenge, N; Erdélyi, R.; Zheng, R.; Korsós, M p-Mode Oscillations in Highly Gravitationally Stratified Magnetic Solar Atmospheres. *Physics* **2022**, *1*, 1–21. https://doi.org/

Received:
Accepted:
Published:

Publisher's Note: MDPI stays neutral with regard to jurisdictional claims in published maps and institutional affiliations.

Abstract: The aim of the work reported in this paper is to gain understanding of solar global oscillations and the propagation characteristics of p-mode oscillations in the highly gravitationally stratified magnetic solar atmosphere. We present a comparison of the analysis of results from observations of ubiquitous intensity oscillations and numerical simulations of potential signatures of global oscillations of the solar atmosphere. 3D numerical magnetohydrodynamic (MHD) simulations of a model solar atmosphere with a uniform vertical cylindrically symmetric magnetic field, employing simulation drivers resulting in oscillations that mimic the behaviour of p-mode oscillations, are presented. The simulations were run for different values of the magnitude of the magnetic field and a p-mode driver with a fixed period of 300 s. For the observational study, a typical active region was selected. We report results for the temporal analysis of the observational data for a region containing a small sunspot (solar pore). The paper reports the variation of the energy flux and oscillation frequency of the magnetosonic modes and examines their dependence on the magnetic field strength. The comparison with observational data indicate the presence of oscillation signals with a frequency close to that measured for the simulated results. We conclude that magnetic regions of the solar atmosphere are favourable regions for the propagation of energy by slow magnetosonic modes. The results exhibit a frequency shift of the oscillations higher in the lower solar atmosphere, for different values of the magnetic field. The numerically obtained periodic behaviour , even in this simplified model atmosphere, is consistent with the observational data, featuring similar frequencies based on the intensity times series of images taken by the Solar Dynamics Observatory.

Keywords: MHD, p-mode, magnetic, solar, atmosphere

1. Introduction

Theoretical and computational studies coupled with observations from solar telescopes, both from ground or space, reveal diverse structures and dynamics in the Sun's atmosphere. The culmination of these studies of the chromosphere and the upper solar atmosphere has enhanced our knowledge of the variety of magnetic field structures. Despite our armoury of observations and the diverse range of computational models it still remains a challenge to make sense of this complex menagerie of dynamical structures, understand solar atmospheric heating (i.e. chromospheric and coronal) and more generally space weather phenomena.

An example of the dynamical complexity are the ubiquitous five-minute oscillations in the lower solar atmosphere (i.e., in particular in the photsophere) that are referred to as the solar global acoustic oscillations or *p*-modes. These global oscillations are interpreted as trapped acoustic waves, i.e. standing acoustic oscillations of the solar interior. Earlier models of these oscillations assumed that there was reflection by the photosphere with at most evanescent propagation above the photosphere. The *p*-modes were interpreted as resonant modes trapped in a cavity formed from the steep change in density at the solar surface and a lower turning point in the interior caused by the increase in the speed of sound resulting in refraction. The physical characteristics of the solar sub-surface layers can be estimated using observations of the standing modes. There is now increasing evidence for leakage of these modes. The complexity and variety of magnetic structures in the solar atmosphere give rise to a mixture of waves providing powerful diagnostics to aid our understanding and advance our knowledge about these structures.

Early theoretical studies reported e.g. in Roberts [42] and Roberts [43] considered wave propagation in idealised magnetic slab structures, demonstrating the fundamental conditions for magnetohydrodynamic (MHD) wave propagation. These models were soon advanced to cylindrical magnetic structures in Edwin & Roberts [14] that addressed which different types of MHD waves can be sustained under the conditions of the solar corona. These papers neglected gravitational stratification and focused on magnetic structuring. There was also an emphasis on the localised wave phenomena. The analysis of Campbell and Roberts [7] investigated the role of horizontal chromospheric magnetic fields for magneto-acoustic modes. As well as finding the shift of frequencies they were also able to predict the circumstances under which different chromospheric regions would either act as a window permitting the propagation of magneto-acoustic energy, a sink where the energy is trapped or reflected back into the chromosphere. The propagation of magneto-acoustic oscillations in an isothermal atmosphere with a vertical magnetic field was investigated by Hindman et al. [27] although small frequency shifts were accounted for, the analysis was unable to demonstrate the absorption of MHD waves, e.g. what is observed in sunspots. Much of the early theoretical (numerical) analyses have focused on the effect of magnetic flux tubes on wave propagation and neglected gravitational stratification. Hasan & Christensen-Dalsgaard [26] considered an isothermal stratified atmosphere and investigated the influence of vertical fields on a variety of modes, including *p*-mode oscillations. In the limit of weak fields, they were able to analyse the spectrum of oscillations in using the modes for a non-magnetised stratified atmosphere and the slow magneto-acoustic mode. The characteristics of generated waves are dependent on the motions at the footpoints of magnetic field concentrations, including those in the intergranular lanes. For example, vortex motions have been demonstrated to generate Alfvén waves Fedun et al. [18].

The link between oscillations in the solar atmosphere and solar global oscillations, what is the topic of the computational modelling work described in this paper, is addressed by Erdélyi [15]. This paper views the photosphere, chromosphere and transition layer as a boundary layer coupling the solar interior and the solar corona. It considers how boundary layers may result in frequency shifts of global oscillations and how it influences the coupling of the internal oscillations with the solar atmosphere.
An outward propagating wave is reflected inward from the solar upper surface, or boundary layer, because of a sudden decrease in the plasma density, while the lower boundary of the cavity is formed by the increasing sound speed due to temperature rises. For global oscillation modes which exceed the acoustic cutoff frequency, there is wave leakage out from the cavity into the atmosphere. A model for understanding the behaviour of solar global oscillations based on the Klein-Gordon equation was further developed by Taroyan & Erdélyi [49]. This model suggests a global resonance. Waves that are normally trapped by a frequency cut-off barrier are enhanced by a resonance enabling propagation into the upper solar atmosphere. The inhomogeneous three-layer model leads to characteristic frequencies. Enhancements to the models described earlier are presented by e.g. Pintér

et al. [40], their work utilised an exponentially decaying horizontal magnetic field as a representation of the magnetic carpet.

For a number of decades, intensity oscillations in the solar atmosphere have been the subject of observation and study, see e.g. the reviews Banerjee et al. [3], De Moortel [11], Mathioudakis et al. [37], Ruderman & Erdélyi [45], Wang [55]. The observed periods of atmospheric intensity oscillations range from a few seconds to several hours Auchère et al. [1]. Much earlier, it was proposed by Jensen & Orrall [29], that the 3- and 5-minute oscillations were the characteristics of the photosphere and the chromosphere. Recently, the association of intensity oscillations with oscillations in coronal loops and sunspots has been confirmed for oscillation periods of three minutes. Applying solar magneto-seismology, observations of intensity observations in the solar atmosphere can be used to understand the magnetic structures in the solar atmosphere, see e.g. Roberts et al. [44], Banerjee et al. [2], Zaqarashvili & Murawski [56], Erdélyi & Taroyan [16], Verth et al. [52]. Additionally, it has been suggested that the 5-minute oscillations in loops may not related to sunspots **?**]. Evidence for global oscillations in the chromosphere, corona is suggested by the observational analysis of Gyenge & Erdélyi [25] demonstrating that the frequent recurrence of micro-flare events exhibit fluctuations between 3 minutes and 12 minutes. These fluctuations arise during time intervals before and after major solar flares.

The key point of this work is a comparison of numerical simulations of a simplified solar atmosphere with observations, searching for a potential link between ubiquitous upper atmospheric oscillations and the global solar oscillations. We use a simple numerical representation that is of sufficient complexity to reveal the dominant dynamical processes in the magnetic solar atmosphere. Comparison of the reported observational work with the results of the modelling provides an indication that the modelling is sufficiently complex to give an insight into the physical mechanisms behind the solar global oscillations. We report the results of numerical simulations of photospheric p-mode oscillations in a model solar atmosphere with a uniform and vertical magnetic field. We also present the results of a temporal analysis based on observations of intensity oscillations with the objective of providing evidence of the existence of the temporal behaviour exhibited by our simulations. The work contributes to our understanding of the propagation and modification of global oscillations in the highly gravitationally stratified solar atmosphere.

First, we consider the variety of magnetic structures in the solar atmosphere and study the wave motions that are observed in these regions. This is followed with a description of the solar atmospheric model, magnetic field configuration and the simulation method we use to compute global oscillations in a magnetic solar atmosphere.

2. Structures in the Solar Atmosphere

The mean photospheric field in the inter-network region is 100-300 G. On the other hand, active regions, containing sunspots that have sizes between 1 - 50 Mm, produce flares that may have fields easily exceeding the range of 100-500 G. As well as these massive concentrations, solar magnetograms reveal a weak-field component, known as the magnetic carpet. These structures are schematically illustrated in Figure 1. Along with the coronal funnels arising from grain boundaries, the picture shows a variety of network loops with temperatures that can be in the range 10^5K to 10^6K. The dynamic phenomena of concern in this paper result in upward waves and oscillations in the solar atmosphere. A spectrum of wave transformation and interaction may occur including reflection and refraction by atmospheric structures.

Our initial computational studies were applicable to quiet Sun regions with magnetic fluxes in the range of 5-10 G, including the non-magnetic solar chromosphere and the quiet inter-network regions between the magnetic flux concentrations. Given the variety of solar atmospheric regions, for example the network, inter network, plage and faculae regions, it is recognised that the modes of oscillation with periods of 3 and 5 minutes exhibit varying behaviour. The variation observed for different magnetic structures and reflecting

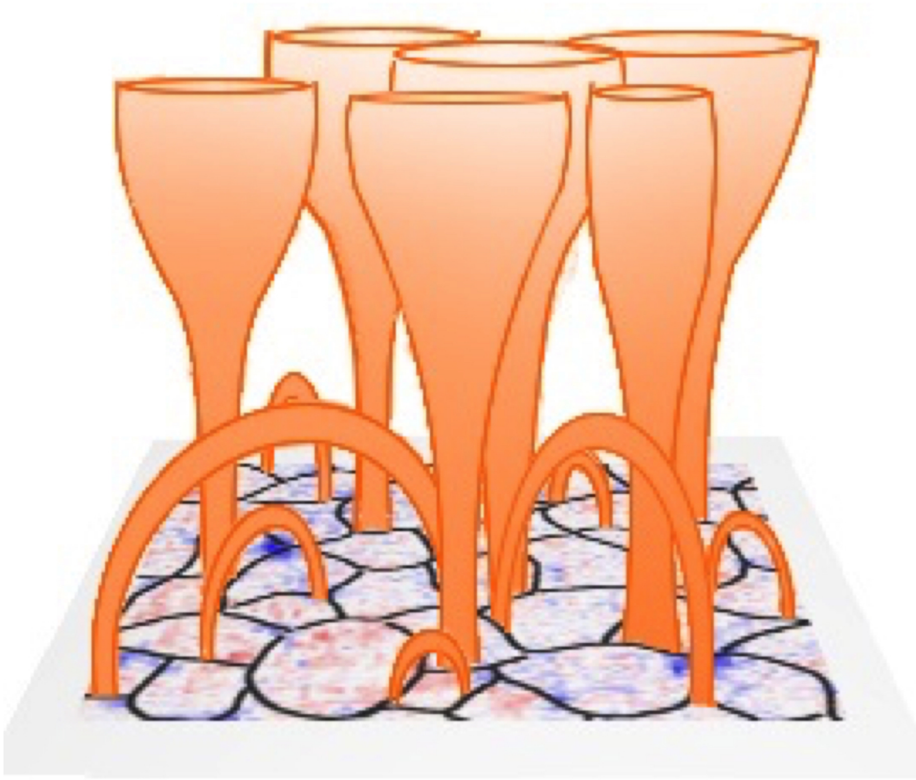

Figure 1. A schematic representation of the solar magnetic network.

layers such as the transition layer influences propagation in the upward and downward directions.

The power spectra presented in the first figure of Griffiths et al. [23] exhibit a variation of propagation characteristics at different levels within the solar atmosphere and within different regions such as coronal holes, the Quiet Sun and active regions. The power spectra indicate a preponderance of long period 5 minute waves with frequencies in the range 1.5-5 mHz. Also observed are the distinctive peaks for the short period 3 minute waves (with frequencies in the range 5-8 mHz). The power spectra exhibit also peaks in much longer period ranges for example 12-minute waves (frequencies in the range 1.1-1.5 mHz) and 16-minute waves (frequencies 1-1.1 mHz). For the Quiet Sun regions the 5 minute modes are stronger at photospheric levels and diminished higher up in the corona, but note a small peak for the data from the AIA 211 corresponding to 2.0MK.

The review of Khomenko and Calvo Santamaria [31] summarises this multifaceted picture. In the close proximity of the magnetic network elements, the longer 5-minute modes propagate efficiently to the chromosphere. The 3-minute modes propagate from the photosphere to the chromosphere in the network cell interiors for restricted regions of the network and internetwork. Although these long-period halos are present in the chromosphere they are most prominent in the photosphere. With their more complex magnetic structures, a more intervened pattern is exhibited in plage and faculae regions. Observations show that the 3-minute modes exhibit enhancement in both photosphere and chromosphere whereas the power of the 5-minute modes increase significantly in the chromosphere. These power enhancements are known as "halos" and have been widely reported Kontogiannis et al. [32].

3. Motivation

Given the complexity of the dynamics and the diversity of structures in the solar atmosphere, it is understood that a truly realistic model is challenging and require a hybrid multi-disciplined approach. A computational MHD simulation of the propagation of waves in 3D solar atmospheres was undertaken by Fedun et al. [17]. Initially they considered hydrodynamical models. In later simulations, Fedun et al. [18] Vigeesh et al. [53] reported results for magnetized solar atmospheres featuring an idealized flux tube. These models with point drivers demonstrated the leakage of magneto-acoustic energy into the solar atmosphere. Many computational MHD simulations of the Sun have been undertaken, some of the approaches have resulted in an encouraging degree of realism Vögler et al. [54], Gudiksen et al. [24]. The work of Khomenko and Calvo Santamaria [31] and Calvo Santamaria, Khomenko and Collados [5] reviewed and presented 2D computational MHD modelling of wave propagation in magnetic features such as sunspots and arcades.

In order to develop a model providing a representation of the solar atmosphere it is necessary to establish that the modelling tools give a consistent behaviour in idealised test cases and that there is a consistency between the computational and theoretical models. Following this principle, an earlier work tested the SMAUG code with hydrodynamic models with drivers representing the standing p-mode oscillations, see Griffiths et al. [23]. A standing mode driver that does not possess any buffeting behaviour, is placed just above the base of the model and mimics the evanescent p-mode oscillation. The study does not consider non-linear effects because the driver we have employed is linear.

The models reveal that vertical magnetic fields enable energy to reach the corona e.g. see Khomenko and Calvo Santamaria [31] and Calvo Santamaria, Khomenko and Collados [5]. Our initial models of a stratified solar atmosphere Griffiths et al. [23] were hydrodynamic simulations. In these simulations, atmospheric perturbations caused by photospheric global oscillations are represented using drivers located in the photosphere so as to mimic the influence of the solar p-modes. The results of the hydrodynamic modelling exhibited agreement with the energy flux predictions from a 2 layer analytical model based on the Klein-Gordon equation. This agreement supported the interpretation of the interaction between the solar atmosphere and the global oscillations. Also revealed by the simulations was a consistency between power flux measurements from SDO and frequency dependent energy flux measurements from the numerical simulations. This observed propagation of energy into the mid to upper atmospheric regions of the Quiet Sun occurred for a range of frequencies. Such observations may explain the observed intensity oscillations for periods greater than the well-known 5-minute and 3-minute oscillations. It was also found that energy flux propagation into the lower solar corona is strongly dependent on the particular wave modes. In this paper, we present the results of investigation into the leakage of energy into the solar atmosphere using 3D numerical MHD simulations with an extended driver representing solar global oscillations.

4. Numerical Computation Methods

The simulations described in this paper were undertaken using the SMAUG code, a GPU implementation of the Sheffield Advanced Code (SAC) Shelyag et al. [47]. The Sheffield MHD Accelerated Using GPUs (SMAUG) Griffiths et al. [20] and SAC are derived from the versatile advection code (VAC) developed by Tóth [50]. SAC and SMAUG are numerical MHD solvers that can be used to model the time-dependent evolution of photospheric oscillations in the solar atmosphere. The SMAUG code can simulate linear and non-linear wave propagation in strongly magnetised plasma with structuring and stratification.

We use the general system of ideal MHD equations applicable to an ideal compressible plasma and used for our initial hydrodynamic simulations, Griffiths et al. [23].

$$\frac{\partial \rho}{\partial t} + \nabla \cdot (\rho \mathbf{v}) = 0, \tag{1}$$

$$\frac{\partial (\rho \mathbf{v})}{\partial t} + \nabla \cdot (\mathbf{v}\rho\mathbf{v} - \mathbf{B}\mathbf{B}) + \nabla p_t = \rho \mathbf{g}, \tag{2}$$

$$\frac{\partial e}{\partial t} + \nabla \cdot (\mathbf{v}e - \mathbf{B}\mathbf{B}\cdot\mathbf{v} + \mathbf{v}p_t) + \nabla p_t = \rho \mathbf{g}\cdot\mathbf{v}, \tag{3}$$

$$\frac{\partial \mathbf{B}}{\partial t} + \nabla \cdot (\mathbf{v}\mathbf{B} - \mathbf{B}\mathbf{v}) = 0. \tag{4}$$

The total pressure p_t is given by

$$p_t = p_k + \frac{\mathbf{B}^2}{2}, \tag{5}$$

and the kinetic pressure, p_k, is written as

$$p_k = (\gamma - 1)\left(e - \frac{\rho \mathbf{v}^2}{2} - \frac{\mathbf{B}^2}{2}\right). \tag{6}$$

In the system of equations above, $\mathbf{B}$ is the magnetic field, $\mathbf{v}$ is the velocity, ρ is the mass density, $\mathbf{g}$ is the gravitational acceleration vector and e is the energy density. The SMAUG code used for the simulations reported here employs perturbed versions of the general set of MHD equations given above. For the perturbed versions the density, energy density and magnetic field are expressed in terms of perturbed and background quantities as follows

$$\rho = \tilde{\rho} + \rho_b,$$
$$e = \tilde{e} + e_b,$$
$$\mathbf{B} = \tilde{\mathbf{B}} + \mathbf{B}_b.$$

Assuming a magneto-hydrostatic equilibrium of the background plasma, the background quantities **that** do not change in time have a subscript b. The time varying perturbed quantities do not have a subscript. The fully non-linear MHD numerical finite element solver employs hyper-diffusion and hyper-resistivity to achieve numerical stability of the computed solution of the MHD equations Caunt and Korpi [9]. A more detailed description of the full set of MHD equations, including the hyper-diffusion source terms are given in Griffiths et al. [20] and Shelyag et al. [47].

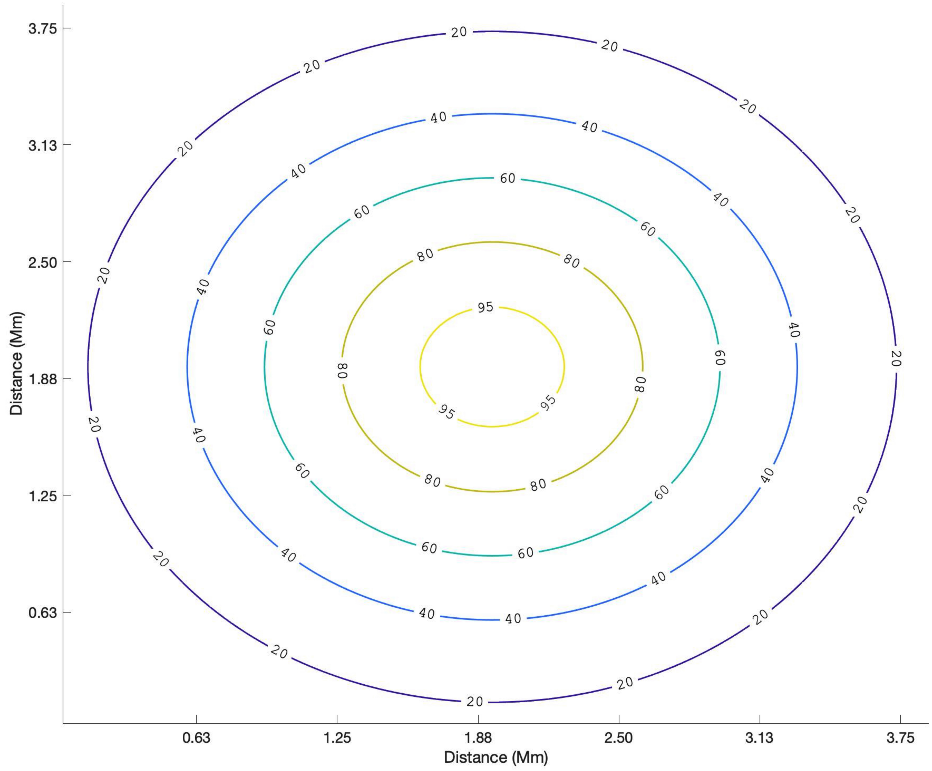

Figure 2. The initial magnetic field configuration showing the radial field distribution **that** is cylindrical and uniform in the vertical direction with a maximum value of 100G.

5. Computational Model 221

The hydrodynamic studies reported in Griffiths et al. [23] employed simulation drivers 222 with physical characteristics representing p-mode oscillations with varying modes and 223 periods. The MHD simulations reported here use the same driver and model of the solar 224 atmosphere as used in our initial hydrodynamic study. The model is **advanced** by the 225 inclusion of a uniform, vertical and cylindrically symmetric magnetic field. 226

The dimensions of the simulation box are $L_x = 4$ Mm, $L_y = 4$ Mm and with a height of 227 $L_z = 6$ Mm in the gravitationally stratified z-direction. The computational box is an array 228 of elements $128 \times 128 \times 128$. The upper boundary of the model is in the solar corona whilst 229 the lower boundary is coincident with the photosphere. The perturbed MHD code used 230 here is suited to studying the propagation of wave energy from the photosphere, across the 231 transition layer and leaking into the solar corona. 232

The time scales relevant to our study are determined by the 5-minute p-mode os- 233 cillations, the model employs boundary conditions allowing us to model induced wave 234 propagation. To generate these oscillations we use vertical velocity drivers **that** are ex- 235 tended across the base of the model. The mechanism for handling the boundaries is crucial 236 for maintaining the stability of a simulation over many cycles of the p-mode oscillation. The 237 challenge is to reduce the reflectivity at the boundaries, in particular, the upper and lower 238 boundaries. The method utilised in these simulations attempts to minimise the gradients 239 near the boundary. Since a central difference method is used to compute the gradients, 240 variable values are copied from the mesh edge into two layers of ghost cells. These layers 241 ensure that the discretization method can be applied over the whole mesh. The net result 242 of this approach is that any generated perturbation will be effectively propagated out of the 243

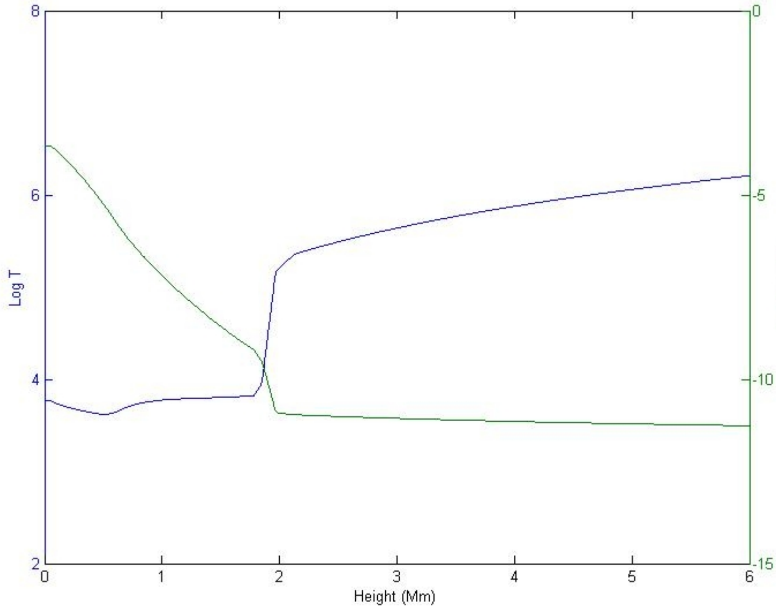

Figure 3. Atmospheric profiles for the density and temperature for the model solar atmosphere based on the VALIIIc model.

computational domain. This type of boundary condition is referred to as an open boundary condition. The following sections describe the model solar atmosphere and the driver.

Data obtained from solar observations were used to construct a semi-empirical model solar atmosphere, the resulting model is a representation of the Quiet Sun. Employing the fundamental assumption of hydrostatic equilibrium, the VALIIIc model Vernazza et al. [51] was used to construct a model of the chromosphere in equilibrium. For atmospheric heights greater than 2.5 Mm the results from a model of solar coronal heating were used McWhirter et al. [38]. The atmospheric profiles for temperature, density, sound speed and frequency cut-off for this model are shown in figure 3 and 4. A further possibility for a model solar atmosphere is the use of parametric models, the smoothed step function used by Murawski and Zaqarashvili [39] is an example. Discussion of the validity of model solar atmospheres and realistic models of the chromosphere, indicate the need for observationally derived semi-empirical models, see Carlsson and Stein [8], Kalkofen [30]. It has been suggested that local dynamo action and joule heating in the dynamical solar chromosphere make the construction of models particularly challenging Leenaarts et al. [34].

For the simulations described here, we use a simplistic model **that** is uniform in the vertical (z) direction. The cylindrically symmetric field was constructed using the parametrisation in equation 7, the effective cylinder radius was fixed at $R = 0.14$Mm. Simulations were run for different values of B_{max}.

$$B_z = B_{max} e^{-\frac{x^2+y^2}{R^2}}. \tag{7}$$

A field configuration with vertical cylindrical symmetry is selected as this provides a working, e.g. rotational symmetry, representation for the weaker intranetwork magnetic field.

Since the field is uniform in the vertical direction the model atmosphere is in magnetohydrostatic equilibrium. This was checked by ensuring that the initial configuration satisfies the magnetohydrostatic balance, for an example see Schüssler and Rempel [46], Gent *et al.* [19]. We also explicitly tested that the there were no dynamic changes in the model due to a magnetohydrostatic imbalance. The resulting density and temperature profiles are shown in Figure 3.

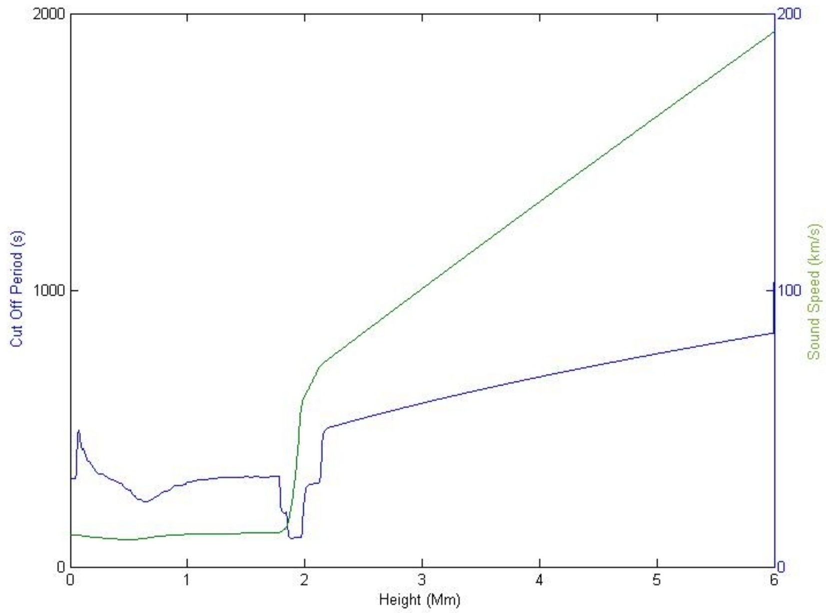

Figure 4. Profiles of the computed speed of sound and the frequency cutoff for a solar model atmosphere based on the VALIIIc model.

6. Numerical Drivers for *p*-mode Oscillations

The work reported here is an extension of the earlier work of Malins [36], their study represented photospheric *p*-mode oscillations using different point drivers. These studies demonstrated the generation of surface waves, structures in the transition zone and identified the effect of cut-offs induced by the stratified solar atmosphere. The brief overview in Section 2 identified physical phenomena delivering energy into the solar atmosphere and resulting in oscillatory behaviour.

The simulations presented in this paper, employ an extended driver resulting in the perturbation of the entire lower boundary of the model. Photospheric *p*-mode oscillations observed for on the Sun have a horizontal wavelength and coherence. The vertical velocity driver used here is an acoustic *p*-mode driver located at the photosphere and exciting waves which propagate into our realistic 3D model of the solar atmosphere. An extended driver with a sinusoidal dependence and a wavelength of 8 Mm applied along the middle of the base of a computational domain of dimension 4 Mm represents a *fundamental mode* component of the global acoustic oscillations. Drivers may be constructed as an ensemble of these solar global eigenmodes. The driver is represented by the expression shown in equation (8)

$$V_z = A_{nm} \sin\left(\frac{2\pi t}{T_s}\right) \sin\left(\frac{(n+1)\pi x}{L_x}\right) \sin\left(\frac{(m+1)\pi y}{L_y}\right) \exp\left(-\frac{(z-z_0)^2}{\Delta z^2}\right), \qquad (8)$$

For the simulations here, a *p*-mode driver corresponding to the 5-minute mode, was used with period 300 s and mode (2,2). Earlier studies demonstrated the effectiveness of this mode with energy propagation, see Griffiths et al. [23]. Simulations were run for different values of the magnitude of the magnetic field. The mode numbers identified here are the n and m values in the expression for the driver shown in Equation (8).

For the driver equation given in Eq. 8, T_s is the period, A_{nm} is the amplitude, the indices n and m define the mode, the lengths of the base of the simulation box in the x and y directions are L_x and L_y are respectively. The driver width, Δz is set to 4 km, the parameter z_0 was set so that the vertical location of the driver is in the photosphere, 0.5 Mm

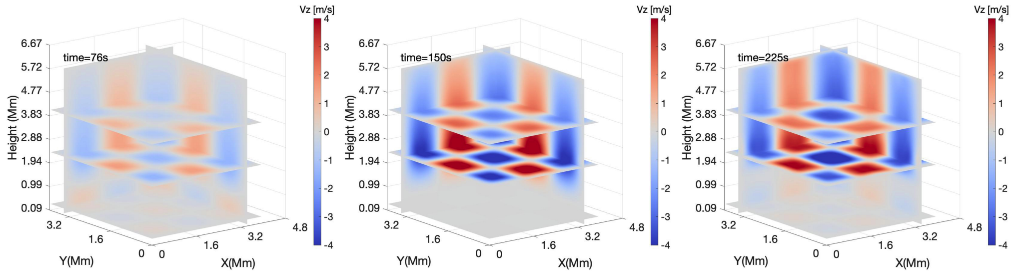

Figure 5. The vertical component of the velocity for different sections of the simulation after different times 76s, 150s and 225s for a vertical field with maximum field of 100G.

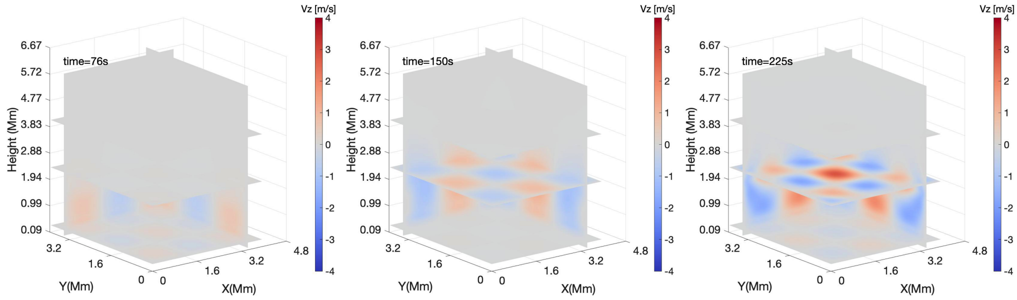

Figure 6. The vertical component of the velocity for different sections of the simulation after different times 76s, 150s and 225s for a magnetic field of 0G.

above the lower boundary of the model and coincident with the location of the temperature minimum. The simulations presented use the parameter A_{nm}=500 ms^{-1} with the mode indices set to $n, m = 2$.

7. Global Magnetoacoustic Waves in Uniform Vertical Magnetic Field Configurations

Magnetohydrodynamic simulations have been performed with p-mode oscillations of the photospheric layer and for magnetic field strengths of 0G, 50G, 75G and 100G. The plasma-β was computed for the case with a magnetic field strength of 100G. The computed plasma-β for the model decreases rapidly from a value of 50 at 0.7Mm above the lower boundary of the simulation domain, β is 1 at a height of 1.39Mm.

Figure 5 shows the vertical component of the velocity at various times for different sections through the simulation box. Each plot in Figure 5 corresponds to a vertical field configuration with a maximum field strength of 100 G. Figure 6 provides a comparison with the 0 G case and illustrates a clear difference between the purely hydrodynamic and the MHD case. The figures for the MHD case exhibit evidence of a fast moving magneto-acoustic wave mode. The measured propagation speed is consistent with that of a fast magneto-acoustic mode. Figures 5 and 6 compare the wave modes at a quarter, half and three-quarters of a cycle.

A set of videos of all the simulations that were performed can be obtained from the online research data archive hosted by The University of Sheffield, Griffiths et al. [22] The videos display the evolution of the z-component of the plasma velocity along different layers of our model solar atmosphere. Each video shows the value of the vertical component of the plasma velocity (z-component in m/s) along different slices through the simulation box. Each video is labelled using the magnetic field strength in Gauss.

Our results indicate that even a small magnetic field appears to enhance the motion of plasma in the corona and there is an apparent difference in phase between the magnetic field cases. As well as an increase in the velocity amplitude with increasing magnetic field there is a small shift in the frequency of the oscillation. In order to fully explain the observed shift further investigative simulations would be required that would include simulations running for a larger number of cycles. The key point here is that the background magnetic field is vertical, one may not accept any frequency shifts assuming a linear wave evolution is the key component to the physics. Since the simulations do show small frequency shifts, this may mean that that the linear theory may break.

After much effort implementing and testing the chosen numerical scheme to solve the numerical equations there are still reflections at the boundary, therefore we consider the simulations to be valid up to the point where reflection occurs, because of this, the simulations are cut after approximately 600 s of real time corresponding to two period cycles.

A time-distance plot for the 300 s period driver, with the 100 G field is shown in Figure 8. The reflections from the imperfect boundary conditions result in increased velocity amplitudes after a few oscillations. Although we are investigating the propagation of waves into the corona, the time-distance plots emphasises phenomena observed in the chromosphere and around the transition zone. The waves speeds measured from this time-distance plot are shown in Table 1. A comparison with the wave speeds computed from the model atmosphere suggests that, the speeds for the 0 G field are consistent with the speed of sound in the solar atmosphere, whilst the speeds for the non-zero magnetic field are consistent with propagation speeds for magnetosonic modes. For a vertical magnetic flux with magnetic field strength B_0 and internal density ρ_0, comparisons with the measured wave speeds were computed using the following definitions: the speed of sound,

$$c_s = \sqrt{\frac{\gamma p_0}{\rho_0}}, \tag{9}$$

the Alfvén speed,

$$v_A = \sqrt{\frac{B_0^2}{\mu \rho_0}}, \tag{10}$$

the magneto-acoustic wave speeds, also known as the slow or tube speed,

$$c_t = \frac{c_s v_A}{\sqrt{(c_s^2 + v_A^2)}}, \tag{11}$$

and the kink speed,

$$c_k = \sqrt{\frac{\rho_0}{\rho_0 + \rho_e}} v_A. \tag{12}$$

The results indicate a variety of waves. Inspection of Figure 8 reveals excitation from the driver along with quasi standing oscillations in the chromospheric cavity. There is also partial reflection of the signal at the boundary of the chromosphere and the transition layer. The results also display evidence for signals propagating horizontally at the transition region and with frequencies similar to that of the driver. The time-distance plot in Figure 7, for the 100 G case, exhibits reduced reflection at the transition layer and indicating energy leakage into the solar corona. Figure 8 shows an initial fast mode pulse followed by slow mode oscillations above the line which corresponds to a plasma-β with a value of one. Below the height of 1 Mm, we observe quasi-standing mode oscillations along with oscillations of the magnetic field perturbations. Below 0.3 Mm, the driver oscillations can be observed in conjunction with possible magneto-acoustic slow mode oscillations. Since the source terms perturb only the vertical component of the velocity and the model is cylindrically symmetric, pure Alfvén modes are not expected.

The time-distance plots and our sections displaying the vertical component of the plasma velocity indicate significant differences in the propagation behaviour for the hydrodynamic and non-zero magnetic field cases. It is necessary to understand and quantify the extent of the energy leakage into the solar atmosphere. To investigate the influence of the magnetic field on the propagation of wave energy we employ an expression for the energy flux which was used by Bogdan et al. [4]. The wave energy flux $\mathbf{F_{wave}}$ is given by

$$\mathbf{F}_{wave} = \tilde{p}_k \mathbf{v} + \tilde{\mathbf{B}} \cdot \mathbf{B}_b \mathbf{v} + \mathbf{v} \cdot \tilde{\mathbf{B}} \mathbf{B}_b.$$

Wave Speed (km/s)	0G	50G	75G	100G
2Mm	12.6	96.5	47.7	25.2
1Mm	10.1	64.1	44.4	45.4
0.5Mm	8.7	45.4	37.8	32.3

Table 1. The table shows wave speeds obtained from the **time-distance** plots for the 300 s period driver with magnetic fields of 0 G,50 G, 75 G and 100 G.

Magnetic Field (G)	1Mm	2Mm	4Mm	5.5Mm
0G	0.155	-1.771 x 10^{-5}	1.227 x 10^{-6}	8.194 x 10^{-7}
50G	0.270	-0.399	0.040	0.021
75G	-0.507	-0.126	0.015	0.007
100G	-0.255	-0.226	0.019	0.006

Table 2. The table shows the time averaged and integrated energy flux ratio obtained for the 300 s period driver with magnetic fields of 0 G,50 G, 75 G and 100 G.

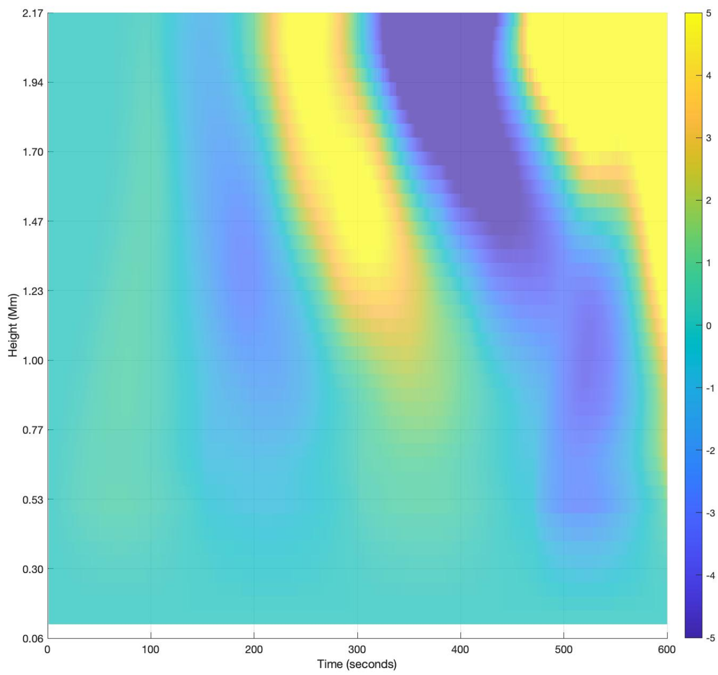

Figure 7. Time-distance plot of the vertical component of the velocity in the mid-chromosphere, for a magnetic field of 0 G.

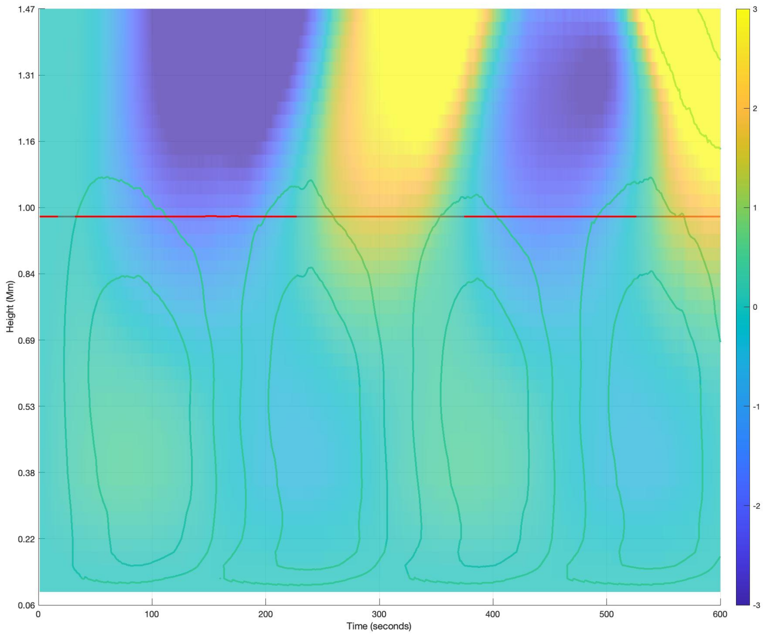

Figure 8. Time-distance plot of the vertical component of the velocity in the mid-chromosphere, for the magnetic field of 100 G, the central red line is the line for plasma-β equal to 1.

We compute the time averaged energy flux integrated over different cross sections of the simulation box.

$$F_{int} = \frac{1}{t_{max}} \int_0^{t_{max}} \int \mathbf{F}_{wave} \cdot d\mathbf{A} dt, \tag{13}$$

These expressions are dependent on the perturbed kinetic pressure $\tilde{p}_k$.

$$\tilde{p}_k = (\gamma - 1)\left(\tilde{e} - \frac{(\tilde{\rho} + \rho_b)\mathbf{v}^2}{2} - \frac{\mathbf{B}^2}{2}\right).$$

Using Equation (13), we computed the energy flux integral for each of the drivers at different atmospheric heights and averaged over the total time. We compute the ratio of this integrated energy flux to the integrated energy flux at the location of the driver. The resulting values are shown in Table 2. It appears that for heights greater than 4 Mm, the energy flux is enhanced for increasing values for the vertical magnetic field. In Figure 9, we plot the ratio of the integrated energy flux ratio for different values of the field at different heights and for the different vertical field values (the blue, orange, purple and red are for field values of 0 G, 50 G, 75 G and 100 G, respectively). These plots demonstrate that for higher B-field magnitudes there is a small leakage of energy propagation. This latter finding is interesting because this is consistent with observations and other simulation results that demonstrate an enhancement for inclined fields.

8. Frequency Analysis

We analyse the temporal behaviour of the numerical result, outlined in the previous section. The top panel of Figure 10 shows a vertical slice of Bz over time. The data is based on the simulation with the initial magnetic field configuration with a maximum value of 100 G. The vertical axis represents the height in Mm and the horizontal axis is the time dimension, measured in seconds. From this 2-dimensional plane, 5 layers were selected, representing different heights in the solar atmosphere. The layers are indicated by

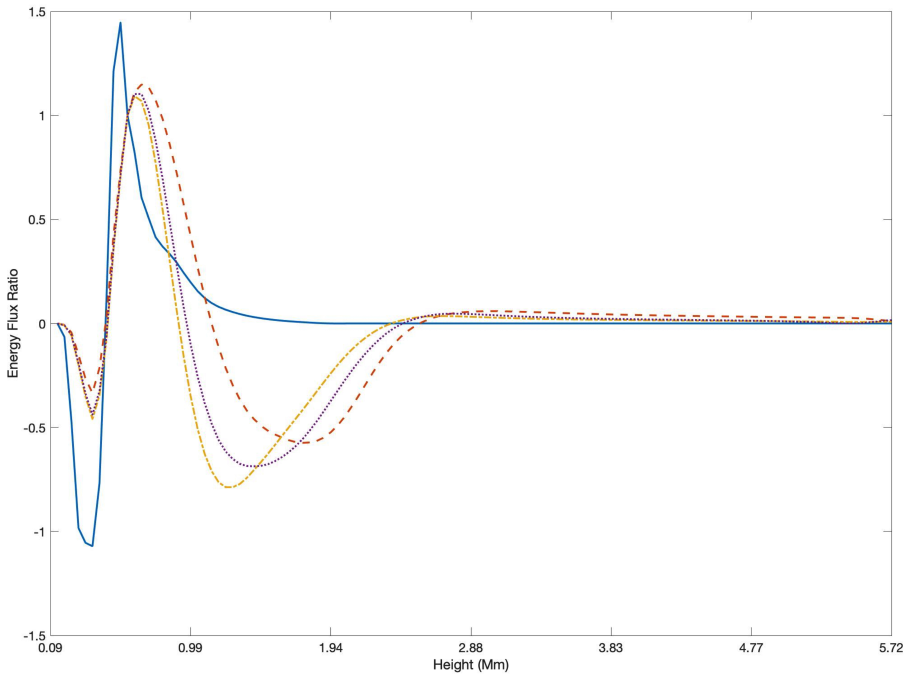

Figure 9. The ratio of the integrated energy flux ratio for different values of the field, blue 0 G, orange 50 G, purple 75 G and red 100 G.

the horizontal grey lines. The middle panel of Figure 10 displays the temporal variation of the selected layers, indicated by different grey shade colours. An FFT was applied (the lower panel of Figure 10) for investigating any oscillatory behaviour in the analysed signal. A significant oscillatory pattern was found with frequency range of 3.75 - 4mHz, corresponding to a period range of 4.2 - 4.4 minutes. A slight frequency shift is also recognisable. The different layers in height tend to feature shifted peaks in FFT. An FFT was also performed based on the other simulations with different initial magnetic field configurations (with a maximum value of 0 G , 50 G, 75 G and 100 G). These investigations all showed similar oscillatory behaviour. Figure 11 features the same analysis as Figure 10, however, the study features a vertical slice of Vz over time. The analysis shows similar properties as the data based on a vertical slice of Bz.

With the objective of confirming the obtained oscillatory behaviour, temporal analysis for the observational data was performed. We investigated intensity oscillations in the solar atmosphere observed by SDO/AIA. The passband 1600 Å was selected because our simulation mainly focused on the lower atmospheric regions, i.e. photosphere and chromosphere. The cadence of 1600 Å images is 24 seconds, therefore it was suitable for studying relatively high-frequency oscillations such as the obtained 4 mHz.

The initial magnetic field configuration of our model is a standing magnetic tube, passing through the chromosphere and the lower corona. Therefore, we randomly chose to sample a typical active region in a simplified way. The selected area contains a small sunspot (solar pore), presumably featuring similar magnetic structure as our simulation. The size of the investigated area covers 50 pixels in total between 18:00 UT to 20:00 UT on 22 August 2010, demonstrated by Figure 13. The obtained time series shows non-stationary behaviour, therefore, the observed linear trend is removed by taking the first difference Δy_t of the data. The first difference is defined as the difference between consecutive observations y_t and y_{t-1}. Furthermore, the times series is also normalised by applying standard scores (Z-scores), defined by:

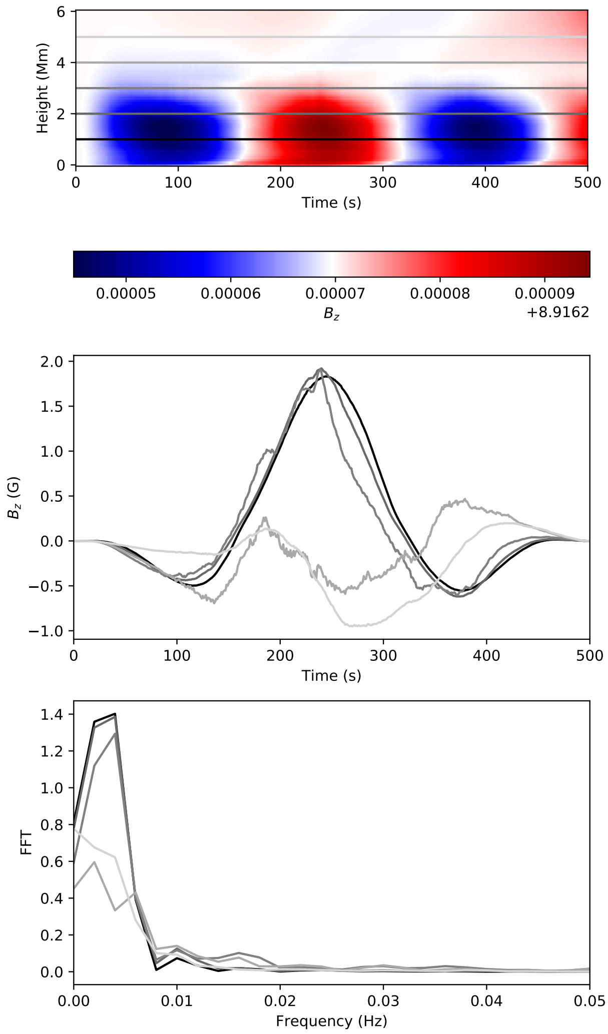

Figure 10. Temporal analysis of B_z vertical slices at 2 Mm. The top panel shows the selected vertical slices, indicated by gray colours. The middle panel demonstrates the obtained signal after applying a Hanning window function. The bottom panel shows the result of the FFT analysis based on the 5 selected vertical B_z slices.

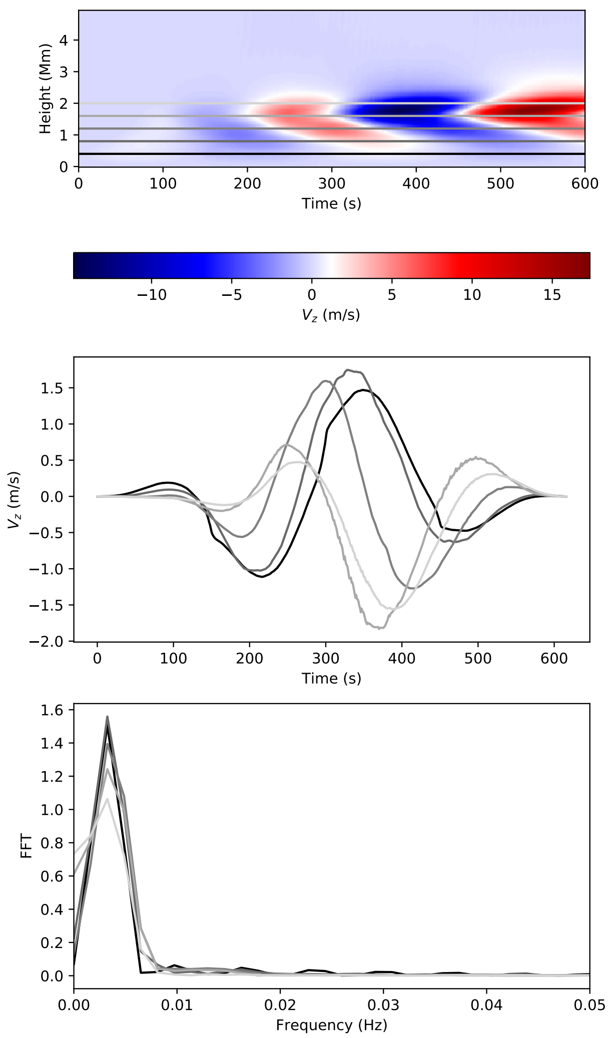

Figure 11. Temporal analysis of V_z vertical slices at 2 Mm. The top panel shows the selected vertical slices, indicated by gray colours. The middle panel demonstrates the obtained signal after applying a Hanning-window function. The bottom panel shows the result of the FFT analysis based on the 5 selected vertical V_z slices.

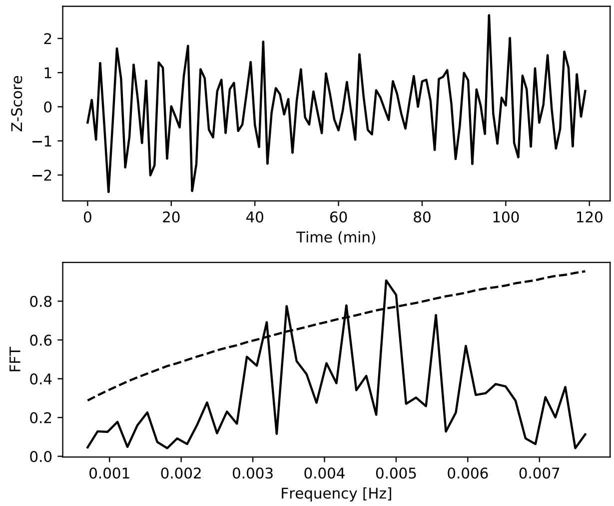

Figure 12. Temporal analysis of the intensity of a 50-pixel large area based on AIA 1600Å between 18:00 UT to 20:00 UT on 22 August 2010. The upper panel shows the temporal variation of the Z-Score (de-trended and normalised pixel intensity data). The lower panel shows the FFT of the analysed observational data.

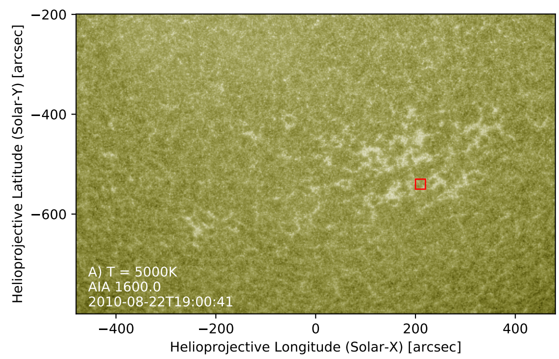

Figure 13. The selected area from the start of the investigate time series at 18:00 UT on 22 August 2010. The area is indicated by red rectangle. The size of the selected area is 50 pixels.

$$Z_i = \frac{T_i - \overline{T}}{\sigma(T)}, \tag{14}$$

where, the parameter $\overline{T}$ is the mean of the time series and the parameter $\sigma(T)$ is defined as the standard deviation of the data. The top panel of Figure 12 demonstrates the trend removed and normalised time series. The lower panel of Figure 11 shows the result of the applied FFT technique. The dashed line is the significance level (3σ) which was calculated using a Monte-Carlo method. The original data showed red noise signature which transformed to blue noise after differentiating the data. We have generated 1 million blue noise signatures N_b and calculated the standard deviation $\sigma(N_b)$ and the mean $\overline{N_b}$ of the simulated noise, providing our significance level S:

$$S = \overline{N_b} + 3\sigma(N_b). \tag{15}$$

A significant period is found with frequency range of $3.5 - 4.2$ mHz , corresponding a period range of 4 - 4.7 minutes, which is close to the period found in simulation data. Another significant peak (5 mHz) is found with period around 3 minutes which may be an indication of another global oscillation. This randomly selected region in the solar surface suggests that the observed oscillation is a global phenomenon.

9. Conclusion

In this paper, we have presented results for a series of MHD simulations of an extended oscillator at the base of a model solar atmosphere. Building upon earlier studies we here extend the modelling to test how the SMAUG code works with an initially symmetric and uniform magnetic field.

We have shown that energy is propagated by magnetosonic modes. Slow and fast magnetosonic modes are responsible for carrying some energy back to the chromosphere and the photosphere. The FFT analysis demonstrated oscillatory patterns with periods in the range 4.2-4.4 minutes. This arose for both the hydrodynamic case and the case with a magnetic field of 100 G. In the latter case there was some additional structure for the FFT analysis. These results compare favourably with the FFT analysis of observations from carefully selected solar features, for example regions with pores. The results exhibit a significant shift of the frequency of these intensity oscillations from the period of the global p-mode oscillation represented in our simulations with a driver of period with 5 minutes. Such shifts may be attributed to additional elasticity in the solar atmosphere resulting from the presence of a magnetic field or from non-linear processes.

Closer inspection of the energy flux propagation results are indicative of enhanced energy flux propagation for increasing magnetic fields. The obtained periodic behaviour is confirmed by observational data, featuring similar frequencies based on the intensity times series of SDO images. The results of the FFT analysis exhibit a difference with the driver frequency. The frequency difference measured from the temporal analysis of the observational and simulation data is larger than would be expected from simple (e.g. linear) theory. This may be linked in part by referring to the work of Campbell and Roberts [7] , however, in their model the magnetic field was horizontal.

The computational results presented here corroborate the suggestion of Didkovsky *et al.* [13] of the existence of global oscillations in the solar corona. The suggestion of small energy deposition events was indicated by Ireland, McAteer, and Inglis [28] in their study of power spectra of the solar corona. They suggest that this is the result of the summation of energy deposition events in the solar atmosphere.

Care must be taken with the measurement of the simulated frequency shifts and further work would investigate more fully the frequency shift mechanism. There are many possible mechanisms, one example could be a result of the superposition of waves arriving at different heights and times such a mechanism allows for the variation of the magnetic field with location and time. Improved boundary conditions handling reflections from the upper boundary may be required to run simulations for much longer time intervals. A further consideration may be a comparison of the results from the vertical tube with a model which is an improved representation of a solar pore Simon and Weiss [48] Cameron *et al.* [6].

It is encouraging that the results presented here, even though the highly idealised approach, are consistent with the behaviour exhibited by earlier work. There is an issue that due to the extended nature of the driver the amplitudes used may be responsible for delivering vast quantities of energy into the solar atmosphere and for driving a highly numerically unstable system and inducing extremely large shocks Calvo Santamaria, Khomenko and Collados [5]. Significant improvements to the comparisons presented in this paper are expected with the recent work of Kostogryz et al. [33]. Here, modelling of intensity perturbations using a VALIIIc solar atmosphere model with radiative transfer the intensity oscillations perturbed by the solar global oscillations modelled using the ADIPLS code of Christensen-Dalsgaard [10]. Also, as described in Rast & Martinez Pillet [41], more sensitive observations with instruments such as DKIST may enable further constraints and the range of theoretical models. Future work will address simulation runs over longer time periods and for inclined fields.

Author Contributions: Conceptualization, R.E., R.Z., N.G. and M.G.; methodology, R.E., N.G. and M.G.; software, M.G. and N.G..; validation, M.G. and N.G.; formal analysis, E.E., M.G. and N.G.; writing—original draft preparation, M.G.; writing—review and editing, R.E., M.G. AND N.G.; visualization, M.G. and N.G.; Preparation of figure 1 and helpful discussion, MK; supervision, R.E.; funding acquisition, R.E. All authors have read and agreed to the published version of the manuscript.

Funding: This research was funded by the UK, Science and Technology Facilities Council (STFC).

Acknowledgments: The authors thank P.H. Keys for providing the wavelet tools to analyse the related SDO data M.B. Korsós for the preparation of Figure 1, the Science and Technology Facilities Council (STFC) of the UK for the support they received (grant number ST/M000826/1). RE acknowledges the support received from the the Royal Society (UK). RE also acknowledges support from the European Union's Horizon 2020 research and innovation programme under the grant agreements no. 739500 (PRE-EST project) and no. 824135 (SOLARNET project). We acknowledge IT Services at The University of Sheffield for the provision of the High Performance Computing Service.

Software: SMAUG, Griffiths et al. [20], SAC Shelyag et al. [47], VAC Tóth [50]

Conflicts of Interest: The authors declare no conflict of interest. The funders had no role in the design of the study; in the collection, analyses, or interpretation of data; in the writing of the manuscript; or in the decision to publish the results.

Abbreviations

The following abbreviations are used in this manuscript:

AIA	Atmospheric Imaging Assembly
FFT	Fast Fourier Transform
GPU	Graphical Processing Unit
MHD	Magnetohydrodynamics
SDO	Solar Dynamics Observatory
SMAUG	Sheffield Magnetohydrodynamics Accelerated Using GPUs
VAC	Versatile Advection Code
VALIIc	Vernazza, Avrett and Loeser

References

1. Auchère, F., Bocchialini, K., Solomon, J., et al. 2014. Long-period intensity pulsations in the solar corona during activity cycle 23. *Astron. Astrophys.*, 563, A8. doi:10.1051/0004-6361/201322572
2. Banerjee, D., Erdélyi, R., Oliver, R., et al. 2007. Present and Future Observing Trends in Atmospheric Magnetoseismology. *Solar Phys.*, 246, 3. doi:10.1007/s11207-007-9029-z
3. Banerjee, D., Gupta, G. R., & Teriaca, L. 2011. Propagating MHD Waves in Coronal Holes. *Space Sci. Rev.*, 158, 267. doi:10.1007/s11214-010-9698-z

4. Bogdan, T. J., Carlsson, M., Hansteen, V. H., McMurry, A., Rosenthal, C. S., Johnson, M., Petty-Powell, S., Zita, E. J., Stein, R. F., McIntosh, S. W., Nordlund, Å., 2003. Waves in the Magnetized Solar Atmosphere. II. Waves from Localized Sources in Magnetic Flux Concentrations. *Astrophys. J.*599, 626–660.
5. Calvo Santamaria, I., Khomenko, E., and Collados, M., 2015. Magnetohydrodynamic wave propagation from the subphotosphere to the corona in an arcade-shaped magnetic field with a null point. *Astron. Astrophys.*577, A70.
6. Cameron, R., Schüssler, M., Vögler, A., and Zakharov, V.: 2007. Radiative magnetohydrodynamic simulations of solar pores. *Astron. Astrophys.***474**, 261. doi:10.1051/0004-6361:20078140.
7. Campbell, W. R. and Roberts, B. 1989. The Influence of a Chromospheric Magnetic Field on the Solar p- and f-Modes *Astrophys. J.*, 338, 538. doi:10.1086/167216
8. Carlsson, M., Stein, R. F., 1995. Does a nonmagnetic solar chromosphere exist? *Astrophys. J. Lett.*440, L29–L32.
9. Caunt, S. E., Korpi, M. J., Apr. 2001. A 3D MHD model of astrophysical flows: Algorithms, tests and parallelisation. *Astron. Astrophys.*369, 706–728.
10. Christensen-Dalsgaard, J. 2008. ADIPLS—the Aarhus adiabatic oscillation package. *Astrophys. Space Sci.*, 316, 113. doi:10.1007/s10509-007-9689-z
11. De Moortel, I. 2009. Longitudinal Waves in Coronal Loops. *Space Sci. Rev.*, 149, 65. doi:10.1007/s11214-009-9526-5
12. De Moortel, I., Ireland, J., Hood, A. W., et al. 2002. The detection of 3 & 5 min period oscillations in coronal loops. *Astron. Astrophys.*, 387, L13. doi:10.1051/0004-6361:20020436
13. Didkovsky, L., Kosovichev, A., Judge, D., Wieman, S., and Woods, T.: 2013. Variability of Solar Five-Minute Oscillations in the Corona as Observed by the Extreme Ultraviolet Spectrophotometer (ESP) on the Solar Dynamics Observatory/Extreme Ultraviolet Variability Experiment (SDO/EVE). *Solar Physics* **287**, 171. doi:10.1007/s11207-012-0186-3.
14. Edwin, P. M. & Roberts, B. 1983. Wave Propagation in a Magnetic Cylinder. *Solar Phys.*, 88, 179. doi:10.1007/BF00196186
15. Erdélyi, R. 2006. Magnetic coupling of waves and oscillations in the lower solar atmosphere: can the tail wag the dog?. Philosophical Transactions of the Royal Society of London Series A, 364, 351. doi:10.1098/rsta.2005.1703
16. Erdélyi, R. & Taroyan, Y. 2008. Hinode EUV spectroscopic observations of coronal oscillations. *Astron. Astrophys.*, 489, L49. doi:10.1051/0004-6361:200810263
17. Fedun, V., Erdélyi, R., Shelyag, S., Sep. 2009. Oscillatory Response of the 3D Solar Atmosphere to the Leakage of Photospheric Motion. *Solar Phys.*258, 219–241.
18. Fedun, V., Erdélyi, R., Shelyag, S., Sep. 2009. MHD waves generated by high-frequency photospheric vortex motions. Annales Geophysicae 29, 1029-1035.
19. Gent, F.A., Fedun, V., Mumford, S.J., and Erdélyi, R.: 2013. Magnetohydrostatic equilibrium - I. Three-dimensional open magnetic flux tube in the stratified solar atmosphere. *Monthly Notices of the Royal Astronomical Society* **435**, 689. doi:10.1093/mnras/stt1328.
20. Griffiths, M. K., Fedun, V., Erdélyi, R., 2015. A Fast MHD Code for Gravitationally Stratified Media using Graphical Processing Units: SMAUG. Journal of Astrophysics and Astronomy 36, 197–223.
21. Griffiths, M., Erdélyi, R., Fedun, V., 2017. Videos of Magnetohydrodynamics Simulations of Solar Atmosphere Wave Dynamics Generated by Solar Global Oscillating Eigenmodes.
https://figshare.com/articles/Videos_of_Magnetohydrodynamics_Simulations_of_Solar_Atmosphere_Wave_Dynamics_Generated_by_Solar_Global_Oscillating_Eigenmodes/4818490
22. Griffiths, M., Erdélyi, R., Fedun, V., 2018. Videos of p-Mode Oscillations in Highly Gravitationally Stratified Magnetic Solar Atmospheres.
https://figshare.shef.ac.uk/articles/dataset/Videos_of_p-Mode_Oscillations_in_Highly_Gravitationally_Stratified_Magnetic_Solar_Atmospheres/7378046
23. Griffiths, M. K., Fedun, V., Erdélyi, R., and Zheng,R., Solar atmosphere wave dynamics generated by solar global oscillating eigenmodes.Advances in Space Research, 61: 720–737, January 2018.
24. B. V. Gudiksen, M. Carlsson, V. H. Hansteen, W. Hayek, J. Leenaarts, and J. Martínez-Sykora. The stellar atmosphere simulation code Bifrost. Code description and validation. *Astron. Astrophys.*, 531:A154, July 2011. doi:10.1051/0004-6361/201116520.
25. Gyenge, N. & Erdélyi, R. 2018 Periodic Recurrence Patterns In X-Ray Solar Flare Appearances. *Astrophys. J.*, 859, 169. doi:10.3847/1538-4357/aac109
26. Hasan, S. S. & Christensen-Dalsgaard, J. 1992. The Influence of a Vertical Magnetic Field on Oscillations in an Isothermal Stratified Atmosphere. *Astrophys. J.*, 396, 311. doi:10.1086/171718
27. Hindman, B. W. and Zweibel, E. G. and Cally, P. S., Mar. 1996. Driven Acoustic Oscillations within a Vertical Magnetic Field. *Astrophys. J.*459, 760–772.
28. Ireland, J., McAteer, R.T.J., and Inglis, A.R.: 2015.Coronal Fourier Power Spectra: Implications for Coronal Seismology and Coronal Heating. *The Astrophysical Journal* **798**, 1. doi:10.1088/0004-637X/798/1/1.
29. Jensen, E. & Orrall, F. Q. 1963. Observational Study of Macroscopic Inhomogeneities in the Solar Atmosphere.IV. Velocity and Intensity Fluctuations Observed in the K Line. *Astrophys. J.*, 138, 252. doi:10.1086/147631
30. Kalkofen, W., 2012. The Validity of Dynamical Models of the Solar Atmosphere. *Solar Phys.*276, 75–95.
31. Khomenko, E., Calvo Santamaria, I., 2013. Magnetohydrodynamic waves driven by p-modes. Journal of Physics Conference Series 440 (1), 012048.

32. I. Kontogiannis, G. Tsiropoula, and K. Tziotziou. Power halo and magnetic shadow in a solar quiet region observed in the Hα line. *Astron. Astrophys.*, 510:A41, February 2010. doi:10.1051/0004-6361/200912841.
33. Kostogryz, N. M., Fournier, D., & Gizon, L. 2021. Modelling continuum intensity perturbations caused by solar acoustic oscillations. *Astron. Astrophys.*, 654, A1. doi:10.1051/0004-6361/202040264
34. Leenaarts, J., Carlsson, M., Hansteen, V., Gudiksen, B. V., 2011. On the minimum temperature of the quiet solar chromosphere. *Astron. Astrophys.*530, A124.
35. Leighton, R. B., 1960. In: Thomas, R. N. (Ed.), Aerodynamic Phenomena in Stellar Atmospheres. Vol. 12 of IAU Symposium. pp. 321–325.
36. Malins, C., 2007. On transition region convection cells in simulations of {p}-mode propagation. Astronomische Nachrichten 328, 752–755.
37. Mathioudakis, M., Jess, D. B., & Erdélyi, R. 2013. Alfvén Waves in the Solar Atmosphere. From Theory to Observations. *Space Sci. Rev.*, 175, 1. doi:10.1007/s11214-012-9944-7
38. McWhirter, R. W. P., Thonemann, P. C., Wilson, R., 1975. The heating of the solar corona. II - A model based on energy balance. *Astron. Astrophys.*40, 63–73.
39. Murawski, K., Zaqarashvili, T. V., 2010. Numerical simulations of spicule formation in the solar atmosphere. *Astron. Astrophys.*519, 9.
40. Pintér, B., Erdélyi, R., & Goossens, M. 2007. Global oscillations in a magnetic solar model. II. Oblique propagation. *Astron. Astrophys.*, 466, 377. doi:10.1051/0004-6361:20041632
41. Rast, M. & Martinez Pillet, V. 2016. Resolving the source of the solar acoustic oscillations: What will be possible with DKIST?. AAS/Solar Physics Division Abstracts #47
42. Roberts, B. 1981. Wave Propagation in a Magnetically Structured Atmosphere - Part One - Surface Waves at a Magnetic Interface. *Solar Phys.*, 69, 27. doi:10.1007/BF00151253
43. Roberts, B. 1981. Wave Propagation in a Magnetically Structured Atmosphere - Part Two - Waves in a Magnetic Slab. *Solar Phys.*, 69, 39. doi:10.1007/BF00151254
44. Roberts, B., Edwin, P. M., & Benz, A. O. 1984. On coronal oscillations. *Astrophys. J.*, 279, 857. doi:10.1086/161956
45. Ruderman, M. S. & Erdélyi, R. 2009. Transverse Oscillations of Coronal Loops. *Space Sci. Rev.*, 149, 199. doi:10.1007/s11214-009-9535-4
46. Schüssler, M. and Rempel, M.: 2005. The dynamical disconnection of sunspots from their magnetic roots. *Astronomy and Astrophysics* **441**, 337. doi:10.1051/0004-6361:20052962.
47. Shelyag, S., Fedun, V., Erdélyi, R., 2008. Magnetohydrodynamic code for gravitationally-stratified media. *Astron. Astrophys.*486, 655–662.
48. Simon, G.W. and Weiss, N.O.: 1970. On the Magnetic Field in Pores. *Solar Phys.***13**, 85. doi:10.1007/BF00963944.
49. Taroyan, Y. & Erdélyi, R. 2008. Global Acoustic Resonance in a Stratified Solar Atmosphere. *Solar Phys.*, 251, 523. doi:10.1007/s11207-008-9154-3
50. Tóth, G., 1996. A General Code for Modeling MHD Flows on Parallel Computers: Versatile Advection Code. Astrophysical Letters and Communications 34, 245.
51. Vernazza, J. E., Avrett, E. H., Loeser, R., 1981. Structure of the solar chromosphere. III - Models of the EUV brightness components of the quiet-sun. Astrophysical Journal Supplement Series 45, 635–725.
52. Verth, G., Erdélyi, R., & Goossens, M. 2010. Magnetoseismology: Eigenmodes of Torsional Alfvén Waves in Stratified Solar Waveguides. *Astrophys. J.*, 714, 1637. doi:10.1088/0004-637X/714/2/1637
53. Vigeesh, G.,Fedun, V.,Hasan, S. S., Erdélyi, R., Jan. 2012. Three-dimensional Simulations of Magnetohydrodynamic Waves in Magnetized Solar Atmosphere. *Astrophys. J.*755, 1–18.
54. A. Vögler, S. Shelyag, M. Schüssler, F. Cattaneo, T. Emonet, and T. Linde. Simulations of magneto-convection in the solar photosphere. Equations, methods, and results of the MURaM code. *Astron. Astrophys.*, 429:335–351, January 2005. doi:10.1051/0004-6361:20041507.
55. Wang, T. 2011. Standing Slow-Mode Waves in Hot Coronal Loops: Observations, Modeling, and Coronal Seismology. *Space Sci. Rev.*, 158, 397. doi:10.1007/s11214-010-9716-1
56. Zaqarashvili, T. V. & Murawski, K. 2007. Torsional oscillations of longitudinally inhomogeneous coronal loops. *Astron. Astrophys.*, 470, 353. doi:10.1051/0004-6361:20077246